Patterns of diel variation in nitrate concentrations in the Potomac River

Douglas A. Burns[1,5], Matthew P. Miller[2,6], Brian A. Pellerin[3,7], and Paul D. Capel[4,8]

[1]US Geological Survey, 425 Jordan Road, Troy, New York 12180 USA
[2]US Geological Survey, 2329 West Orton Circle, West Valley City, Utah 84119 USA
[3]US Geological Survey, 12201 Sunrise Valley Drive, Room 5A116, MS 412, Reston, Virginia 20192 USA
[4]US Geological Survey, 122 Civil Engineering Building, 500 Pillsbury Drive SE, Minneapolis, Minnesota 55455 USA

Abstract: The Potomac River is a large source of N to Chesapeake Bay, where reducing nutrient loads is a focus of efforts to improve trophic status. Better understanding of NO_3^- loss, reflected in part by diel variation in NO_3^- concentrations, may refine model predictions of N loads to the Bay. We analyzed 2 y of high-frequency NO_3^- sensor data in the Potomac to quantify seasonal variation in the magnitude and timing of diel NO_3^- loss. Diel patterns were evident, especially during low flow, despite broad seasonal and flow-driven variation in NO_3^- concentrations. Diel variation was ~0.01 mg N/L in winter and 0.02 to 0.03 mg N/L in summer with intermediate values in spring and autumn, equivalent to <1% of the daily mean NO_3^- concentration in winter and ~2 to 4% in summer. Maximum diel NO_3^- values generally occurred in mid- to late morning, with more repeatable patterns in summer and wider variation in autumn and winter. Diel NO_3^- loss reduced loads by 0.7% in winter and 3% in summer. These losses were less than estimates of total in-stream NO_3^- load loss across the basin that averaged 33% of the annual groundwater contribution to the river. Water temperature and discharge had stronger relationships to the daily magnitude of diel NO_3^- variation than did photosynthetically active radiation. Estimated diel areal NO_3^- loss rates were generally >1000 mg N m^{-2} d^{-1}, greater than most published values because measurements in this large river integrate over a greater depth/unit stream bottom area than do those from smaller rivers. These diel NO_3^- patterns are consistent with the influence of photoautotrophic uptake and related denitrification, but we cannot attribute these patterns to assimilation alone because the magnitude and timing of diel dynamics were affected to an unknown extent by processes, such as evapotranspiration, transient storage, and hydrodynamic dispersion. Improvements to diel loss estimates will require additional high-frequency measures, such as dissolved O_2, dissolved organic N, and NH_4^+, and deployment of 2 measurement stations.

Key words: nitrogen, nitrate, diel variation, Potomac River, Chesapeake Bay, in-stream loss

Human activities, such as agriculture and the combustion of fossil fuels, have increased the global production of reactive N by >10× since the mid-19th century (Galloway et al. 2008). This enhanced production of reactive N has resulted in large increases in food and energy production, but also has led to large increases in environmental fluxes and stores of various N forms, which in turn, have led to a cascade of environmental and human health concerns (Galloway et al. 2003). One of these concerns is the increased transport of N by rivers to coastal estuaries, which may enhance biological production and lead to eutrophication and associated hypoxia with implications for water clarity and the aquatic food web (Bricker et al. 2008). The Chesapeake Bay provides a well-studied example of how increases in riverine N loads associated with human activities over the past century have led to a wide array of environmental effects with deleterious economic consequences for fisheries (Kemp et al. 2005).

Widespread recognition of the role of human activities as drivers of estuarine eutrophication through enhanced delivery of N and other nutrients by rivers has led to efforts to improve agricultural management practices to reduce the delivery of these nutrients to estuaries, such as the Chesapeake Bay, Mississippi River Embayment, Tampa Bay, and others (Bricker et al. 2008). To track the success of nutrient reduction strategies and to calibrate and validate models that can help identify key biogeochemical processes and make predictions of potential future conditions, increased

E-mail addresses: [5]daburns@usgs.gov; [6]mamiller@usgs.gov; [7]bpeller@usgs.gov; [8]capel@usgs.gov

DOI: 10.1086/688777. Received 9 November 2015; Accepted 9 June 2016; Published online 8 September 2016.
Freshwater Science. 2016. 35(4):1117–1132.

research efforts and environmental monitoring of N and other nutrients have been implemented in estuaries, such as the Chesapeake Bay (http://www.chesapeake.org/stac/).

A key aspect of the movement of N from terrestrial soils to estuaries is the role of in-stream and near-stream biogeochemical and hydrologic processes during N transport in the river network (Birgand et al. 2007). A variety of processes, including denitrification, nitrification, biological assimilation, and mixing and hydrologic exchange with groundwater, inflowing tributaries, and point sources of discharge, can increase or decrease concentrations of various forms of N during river transport (Triska et al. 1989, Hall et al. 2009, Mulholland et al. 2009). Most investigations of in-stream N dynamics have focused on small streams, in part because of the ease with which study approaches, such as mass balance and tracer injections, can be applied in such systems. However, several investigators focused on larger rivers and generally concluded that these systems have an intrinsic capacity to remove a large proportion of the N load that would otherwise be transported downstream to estuaries (Wollheim et al. 2006, Tank et al. 2008). Most streams and rivers are net sinks of N because of widespread denitrification and assimilation (Laursen and Seitzinger 2004, Hall et al. 2009, Mulholland et al. 2009). Watershed N models generally reflect the importance of in-stream loss processes (Preston et al. 2011, Worrall et al. 2012). Model results from the Potomac River, a major tributary of the Chesapeake Bay, indicate large in-stream losses during transport (Miller et al. 2016) that may exceed ½ of the N that enters the river network (Seitzinger et al. 2002). These losses increase with increasing water temperature across a wide spatial range of stream reaches (Ator et al. 2011).

In-stream N loss rates can vary with season, concentration, and other factors (Smith et al. 2008, O'Brien and Dodds 2010), but data available to evaluate and model in-stream losses are limited (Wollheim et al. 2006). Therefore, many models use fairly simple approaches to estimate in-stream loss and do not explicitly consider temporal variation (Alexander et al. 2000, Seitzinger et al. 2002, Worrall et al. 2012).

Diel cycling of NO_3^- concentrations has been observed in many streams and rivers (Burns 1998, Roberts and Mulholland 2007, Heffernan and Cohen 2010), although not all systems show diel patterns (Pellerin et al. 2014). Diel variation may reflect assimilation by the autotrophic community during daylight hours and cessation during dark hours when respiration is dominant (Heffernan and Cohen 2010). These patterns also might reflect links to heterotrophic assimilation and denitrification through photosynthetically driven diel variation in the availability of autochthonous labile C (Holmes et al. 1996) or might reflect the effects of the daily cycle of evapotranspiration on the near-stream hydraulic gradient and resulting inflow rate of ground water (Flewelling et al. 2014). Regardless of the direct and indirect processes that control diel variation in NO_3^- concentrations, the timing, magnitude, and seasonal variation of diel patterns provide a fundamental measure of an aspect of the capacity of a river to diminish NO_3^- during downstream transport. A caveat is that NO_3^- losses, as reflected by diel patterns, may represent only temporary loss because assimilated NO_3^- can be re-released back to the water column through a variety of processes (von Schiller et al. 2015).

The Potomac River is the 2nd-largest tributary to the Chesapeake Bay and is a major source of N and other nutrients to the estuary (Boynton et al. 1995, Sprague et al. 2000, Ator et al. 2011). NO_3^- is the dominant N form in the river, equivalent to ~⅔ of the total N load (Blomquist et al. 1996). In late 2011, a sensor capable of frequent NO_3^- measurements was installed in the Potomac River, just upstream of tidal influence at Little Falls, Maryland. The data from this sensor have provided an unprecedented opportunity to gain insight into the role of in-river processes in N transport to the Bay (Miller et al. 2016), particularly the role of processes reflected in the diel variation of NO_3^- in the river. The objective of our study was to describe seasonal patterns of diel variation in NO_3^- concentrations in the Potomac River, including the magnitude and timing of these patterns, to explore the physical factors that may control temporal variation in diel patterns, and to estimate the contribution of diel NO_3^- variation to total in-river losses of NO_3^- during transport in the river network. Our goal was to provide an approach for analyzing these diel patterns that could be applied by other investigators and lead to improved understanding of controls on the transport of NO_3^- by rivers to estuarine ecosystems.

METHODS

Study site

The study site is the Potomac River gage near Washington, DC, at the Little Falls Pump Station (US Geological Survey [USGS] ID = 01646500), a 29,940 km^2 basin (Fig. 1). This basin is commonly referred to as the Upper Potomac River in assessments of the Chesapeake Bay (Bricker et al. 2014). The Upper Potomac basin encompasses diverse geomorphic settings including the Appalachian Plateau, Valley and Ridge, Blue Ridge, and Piedmont physiographic provinces in Maryland, Pennsylvania, Virginia, and West Virginia (Ator et al. 1997). About 60% of the basin is forested land, and agricultural land occupies ~35% of the basin (Bricker et al. 2014). This agricultural land is the dominant source of N in the basin, and provided 64% of the total river N load in 2002 (Ator et al. 2011). Urban land, while composing <3% of the Upper Potomac basin, has been increasing in recent years, and contributes ~11% of the total N load to the river. Atmospheric deposition provides ~18% of

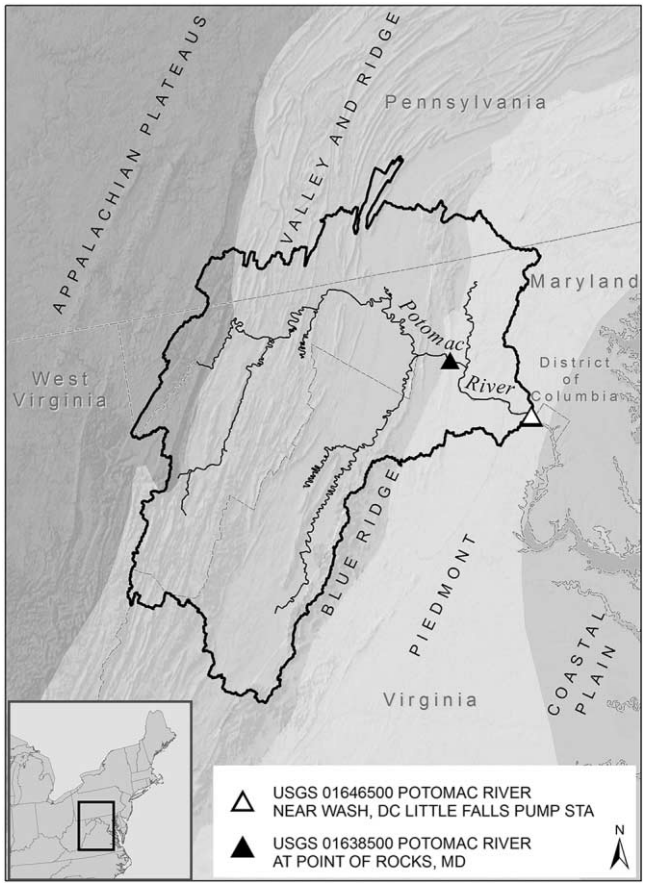

Figure 1. Potomac River watershed with US Geological Survey gages at Little Falls and Point of Rocks shown.

the total N load to the basin (Ator et al. 2011), but this source has decreased recently, and the decrease may be responsible in part for observed declines in river N loads (Eshleman et al. 2013). Point sources provide ~4 to 7% of the N load to the river at the Little Falls gage (Blomquist et al. 1996, Ator et al. 2011). Contributions from point sources have been decreasing in recent years because of upgrades to wastewater treatment facilities (Woods et al. 2013), which probably are contributing to downward trends in N loads to the Chesapeake Bay. All data files that were used in the analyses described in our paper can be downloaded from: https://doi.org/10.5066/F7HT2MD4.

Sensor measurements

A Submersible Ultraviolet Nitrate Analyzer (SUNA) with a 10-mm optical path length (version 1; Satlantic, Nova Scotia, Canada) was deployed to collect high-frequency NO_3^- measurements. The SUNA sensor was mounted on an instrument cage and fixed vertically on the left bank of the river. Specific conductance, pH, and temperature (at 3 depths) were measured at this site (6-Series multi-parameter sonde; Yellow Springs Instruments, Yellow Springs, Ohio). The sensor array was immediately adjacent to the gage where river stage was recorded every 15 min for conversion to discharge by applying a stage–discharge relation according to standard USGS methods (Rantz et al. 1982).

High frequency NO_3^- data were collected every 15 min during the period 1 December 2011 to 30 November 2013 with the SUNA operated in freshwater mode (i.e., without bromide temperature compensation). The instrument was equipped with an external nylon brush wiper (Zebra-Tech, Nelson, New Zealand) that cleaned the optical window prior to each sampling interval. The sensor was checked for blanks and linearity prior to and during deployment as described by Pellerin et al. (2013).

River NO_3^- concentrations were measured by the SUNA at a sampling rate of ~1 Hz over a 30-s burst window at each sampling interval, which typically resulted in ~20 measurements of NO_3^- concentrations per burst. Outliers within the burst were eliminated based on the median absolute deviation, and burst statistics (mean, median, and standard deviation [SD]) were calculated from the remaining data (typically >90% of the initial burst data). Additional information that describes the burst variability and spectral data, such as the root mean square error (RMSE) of the algorithm fit, were used to flag erroneous data from the time series (Pellerin et al. 2013), and resulted in elimination of ~2% of the data from the record. Accuracy of the SUNA sensor in freshwater applications, such as the Potomac River, is ~±0.03 mg/L NO_3^--N, and short-term precision is ~0.004 mg/L NO_3^--N (Satlantic 2014).

A regression of depth- and width-integrated discrete samples (n = 43) that were collected during the study period ~2 km downstream of the gage and analyzed for NO_3^- + NO_2^- concentrations with simultaneous sensor NO_3^- concentrations indicated that the 2 sets of measurements were strongly correlated with little bias (r^2 = 0.98, slope = 0.98, y-intercept = 0.018) (Fig. S1). The SUNA does not explicitly account for absorbance by NO_2^- in the range of 210–220 nm, but the concentration of NO_2^- is almost always negligible in surface waters and has little effect on reported N concentrations (National Research Council 1995). Therefore, hereafter the sensor measurements are referred to as NO_3^- in units of mg N/L. These sensor measurements are publically available from: http://waterdata.usgs.gov/md/nwis/uv?site_no=01646500.

Data preparation

A daily record for analysis of diel variation in NO_3^- concentrations during December 2011 through November 2013 was developed in 2 steps: 1) elimination of days with excessive missing values, and 2) elimination of data that did not show diel variation. Step 1 involved eliminating days in which the cyclical maximum and minimum

NO_3^- concentrations could not be identified because of excessive missing values. Values were missing because of instrument malfunction or excessive sediment loads when the instrument failed to produce a value. For days that had only a small proportion of missing values (generally <10–20% without long consecutive gaps), linear interpolation was applied to fill in data gaps to allow accurate calculation of the moving average that was applied in data analyses. Step 1 resulted in the elimination of 65 d from further consideration.

Step 2 included an automated approach combined with visual inspection of the NO_3^- chemograph and the river hydrograph to eliminate days during which a clear pattern of diel variation in NO_3^- concentrations was not evident. Diel variation could not be identified during and immediately after precipitation events when NO_3^- concentrations showed strong excursions before returning to a diel pattern during the hydrograph recession. Removal of days when these large variations in NO_3^- concentrations prevented evaluation of a diel pattern means that our analysis is biased toward low and moderate flow conditions. The extent to which diel variation may have affected NO_3^- concentrations during and immediately after storms could not be assessed with the analysis approach applied here.

A digital filter hydrograph separation approach was applied as described by Lim et al. (2005; BFLOW; available at: https://engineering.purdue.edu/~what/) to evaluate high-flow days for potential removal. This program separates the hydrograph into direct runoff and baseflow components and is a convenient, objective, and reproducible empirical approach for distinguishing rapid runoff from baseflow. Days in which direct runoff was >20% of streamflow were considered candidates for removal, but first were checked visually by examining graphs of river discharge (Q) and NO_3^- concentrations. Small precipitation events sometimes resulted in little change in NO_3^- concentrations and were insufficient to halt diel variation. Therefore, these days were not removed prior to analysis. In contrast, large storms sometimes disrupted diel variation patterns for several days after the hydrograph peak. Some days with direct runoff <20%, particularly during hydrograph recessions, were removed prior to analysis based on visual inspection. Step 2 resulted in elimination of 129 d from further analysis. This final step resulted in a data set of 537 d available for analysis over the 2-y study period. The seasonal division in the analysis was: winter (21 December–20 March) = 116 d, spring (21 March–20 June) = 138 d, summer (21 June–20 September) = 153 d, and autumn (21 September–20 December) = 130 d.

Data analysis

A 5-sample moving-average NO_3^- concentration was calculated to minimize the influence of signal noise in the analysis. These moving-average values were the basis for all analyses described herein. Before eliminating missing or storm-influenced data as described above, a Loess smooth was applied to 30-d data windows. Loess is a weighted regression-based smoothing approach (Cleveland and Devlin 1988). In this case, a 1st-order polynomial regression was applied using a tricube weighting function applied to 6% of the data window (~1-d smoothing window). The smooth provided a reference level from which the time of the daily NO_3^- maximum and minimum values could be identified (as shown in Fig. 2). The timing of these maximum and minimum diel NO_3^- concentrations was summarized across seasons as standardized z scores. The z score was calculated as $z = x - \mu/\sigma$, where x is each measurement, μ is the mean for each day, and σ is the SD of the mean. The application of the smooth to provide a daily reference level was necessary because the maximum and minimum diel NO_3^- values did not always equate to the maximum and minimum concentrations in a given day when NO_3^- was undergoing multiday increases or decreases associated with seasonal or multiday sources of variation.

The magnitudes of daily NO_3^- variation and loss were calculated by connecting the daily NO_3^- maxima with a linearly interpolated line and calculating the maximum and mean daily difference of this line from the sensor NO_3^- concentrations (Fig. 2). This approach is similar to the

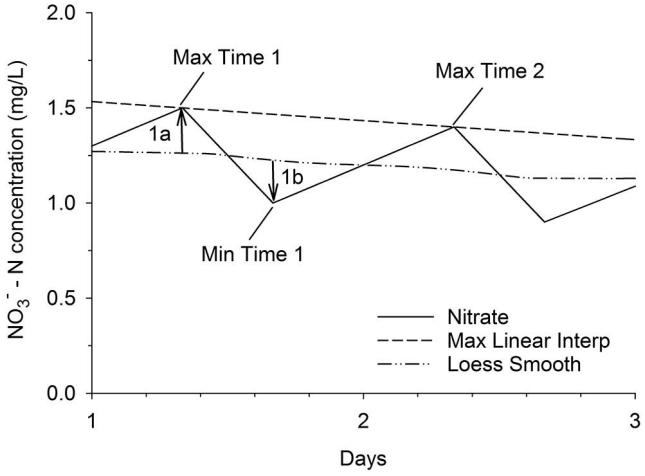

Figure 2. Idealized representation of 2 d of NO_3^- sensor data to illustrate how the times of maximum (max) and minimum (min) diel NO_3^- concentrations and NO_3^- loss were identified. The time of maximum diel NO_3^- concentration was identified as the point on the NO_3^- sensor line at which the length of arrow 1a was at a maximum on each day. The time of minimum diel NO_3^- concentration was identified as the point at which the length of arrow 1b was at a maximum on each day. The concentration difference between the max linear interpolated (interp) line and the sensor NO_3^- line as identified by the sum of the lengths of arrows 1a and 1b provided the daily maximum diel NO_3^- concentration loss. The daily mean diel NO_3^- concentration loss was calculated as the mean difference between the max linear interpolated line and the sensor NO_3^- line within the triangle formed by Max Time 1, Min Time 1, and Max Time 2.

2nd method for calculating autotrophic NO_3^- assimilation described by Heffernan and Cohen (see fig. 1B by Heffernan and Cohen 2010). The daily mean diel NO_3^- concentration loss was calculated as:

$$\text{Daily mean diel } NO_3^- \text{ concentration loss} = \sum(NO_3^-{}_{max} - NO_3^-{}_i)/96, \quad \text{(Eq. 1)}$$

for i = 1 to 96, where $NO_3^-{}_{max}$ is the NO_3^- concentration (mg N/L) of the interpolated line that connects daily maximum values at each 15-min interval (Fig. 2) and $NO_3^-{}_i$ is the NO_3^- concentration at each 15-min interval. The daily maximum diel NO_3^- concentration loss was the maximum value of $NO_3^-{}_{max} - NO_3^-{}_i$ on each day. The daily mean and maximum diel NO_3^- concentration loss also were expressed as monthly and seasonal mean values and as a percentage of the cumulative value of $NO_3^-{}_{max} - NO_3^-{}_i$ on each day. Daily mean and maximum diel NO_3^- load loss was calculated in a manner similar to the calculation of concentration loss by multiplying each NO_3^- concentration by Q in units of L/15 min.

Several physical measures were explored for their strength of association with the magnitude of diel NO_3^- loss and the timing of diel maximum and minimum NO_3^- values by calculating Pearson product–moment correlations. The time of maximum and minimum diel NO_3^- concentrations were converted to Cartesian coordinates and an approach for calculating the linear association between a circular and linear variable was applied (Zar 1999). The physical measures included daily mean: water temperature, Q, and photosynthetically active radiation (PAR). Q and water temperature are measured at the Potomac River at Little Falls stream gage by the USGS (data available from: http://waterdata.usgs.gov/md/nwis/uv?site_no=01646500). Several additional metrics were derived from daily mean Q to allow consideration of antecedent and threshold effects, including days since Q exceeded thresholds of 283 m^3/s, 425 m^3/s, and 566 m^3/s (representing flow exceedance values of ~65, 80, and 90%, respectively), and 1, 3, 5, 7, 10, and 14-d mean antecedent Q.

PAR was not measured at the Potomac stream gage, but these data were available at 3-min intervals from the US Department of Agriculture Research Station in Beltsville, Maryland, ~ 22 km from the stream gage (data available at: http://uvb.nrel.colostate.edu/UVB/index.jsf). Several threshold and antecedent metrics were derived from these data including mean, median, maximum, 10th, 25th, 75th, and 90th percentile for each day, and 1-, 3-, 5-, 7-, 10-, and 14-d mean antecedent values. In addition to the correlations of these physical measures with diel NO_3^- loss, various combinations of these measures were explored for their ability to explain variation in the magnitude of diel NO_3^- loss through forward stepwise multiple linear regression (Appendix S1).

Daily areal NO_3^- loss rate was estimated as:

$$\text{Daily areal loss rate} = (Q/WV)\sum(NO_3^-{}_{max} - NO_3^-{}_i), \quad \text{(Eq. 2)}$$

for i = 1 to 96, where Q = river discharge (m^3/15 min), W = river channel width (m), V = river velocity (m/15 min), $NO_3^-{}_{max}$ and $NO_3^-{}_i$ are as shown previously except in units of mg/m^3. This quantity can be viewed as an estimate of the daily net areal loss rate of NO_3^- that results from all processes that contribute to diel NO_3^- variation. These processes include direct assimilation from the water column and indirect processes, such as denitrification, that may be driven in part by assimilation. The term 'loss' rather than uptake or assimilation as applied in other analyses is used here because of the potential and unquantified effects of hydrologic processes, such as hydrodynamic dispersion and transient storage, on the magnitude of these diel patterns. This estimate of loss is similar to equation 2 by Heffernan and Cohen (2010) with 2 exceptions: 1) here effective river bed or river surface area was assumed to be a dynamic quantity, and 2) WV replaces riverbed area in our calculation. It follows that the effective area of the river reach assumed to influence diel NO_3^- loss varies with V and W. A 1-d travel distance was calculated by multiplying V in Eq. 2 by 96, and is based on the assumption that V is representative of the entire reach.

Highly accurate Ws and Vs for calculating daily NO_3^- loss rates would require detailed measurements of these quantities at several locations along a river reach that represents 1 d of travel time upstream of the Little Falls gage. These measurements would be needed over a range of flow conditions because W and V vary with Q. Such detailed data were not available. However, W and V have been measured repeatedly to define the stage–discharge relationship at the Little Falls gage and at the Point of Rocks gage (USGS ID = 01638500), ~66 km upstream, a travel time of 13 to 63 h over the range of flow represented by the current analysis (Searcy and Davis 1961). Mean W between these 2 gages was estimated to be 379 m based on the polygon representing the river channel as obtained from the high-resolution National Hydrography Dataset (http://nhd.usgs.gov/data.html). Ws measured at Point of Rocks provided a better representation of this mean W because the mean width at the measurement section for this gage was 279 m based on 176 measurements during 1905 to 2012. In contrast, the measurement section at Little Falls is narrow and deep with a mean width of 55 m based on 177 measurements during 1930 to 2012. Therefore, W and V measurements from Point of Rocks were applied to estimate diel areal NO_3^- loss rates for the relevant reach. The measurements at Point of Rocks showed a strong regression relationship between W and Q ($W = 177.58Q^{0.0896}$, $p < 0.001$, $r^2 = 0.58$) and between V and Q ($V = 0.275 + 0.00144Q + 0.000000534Q^2$, $p < 0.001$, r^2 =

0.92). These regressions were applied to provide estimates of W and V as a function of Q to calculate diel areal NO_3^- loss rates according to Eq. 2. The daily mean V was also used to calculate a 1-d travel time that represents the approximate reach length along the main channel over which processes that affect the diel variation in NO_3^- concentrations are thought to have influence.

Daily areal loss rates (mg N m^{-2} d^{-1}) reflect estimates of the effects of all processes that result in diel variation of NO_3^- in the Potomac River. Diel NO_3^- variation may reflect the net effects of several different processes including autotrophic uptake, denitrification, nitrification, hydrodynamic dispersion, and anthropogenic withdrawals or additions to the river. Given the diverse and large Potomac basin, we are not able to attribute NO_3^- losses to any particular process, so these rates should be viewed as a metric that reflects the net effects of all processes that act to affect diel variation in NO_3^- concentrations in this system.

Daily mean and maximum diel NO_3^- load losses were compared on a seasonal basis to daily total basin in-stream and near-stream (post-terrestrial processing, but including the hyporheic zone) NO_3^- losses by applying an approach developed by Miller et al. (2016). In this approach, the river NO_3^- load was assumed to reflect the following mass-balance expression that was solved on a daily basis:

$$NO_3^-{}_{in} Q_{stream} = NO_3^-{}_{GWD} Q_{GWD} + NO_3^-{}_{RO} Q_{RO}, \quad \text{(Eq. 3)}$$

where $NO_3^-{}_{in}$ is the NO_3^- concentration resulting from the combined transport of $NO_3^-{}_{GWD}$ and $NO_3^-{}_{RO}$ to the river, Q_{stream} is river discharge, $NO_3^-{}_{GWD}$ is the NO_3^- concentration transported to the river as groundwater, Q_{GWD} is discharge of water to the river as groundwater, $NO_3^-{}_{RO}$ is NO_3^- concentration transported to the river as runoff, and Q_{RO} is discharge of water to the river as runoff. Loss or gain in NO_3^- concentration was then calculated as:

$$NO_3^-{}_{proc} = NO_3^-{}_{in} - NO_3^-{}_{meas}, \quad \text{(Eq. 4)}$$

where $NO_3^-{}_{proc}$ = the net loss (+) or gain (–) in NO_3^- concentration resulting from in-stream biogeochemical processes and $NO_3^-{}_{meas}$ is daily mean NO_3^- concentration in the river. Q_{GWD} and Q_{RO} were calculated through a graphical hydrograph separation using a digital-filter approach (Eckhardt 2005) with the backward filtering method of Collischonn and Fan (2013), and Q_{stream} was the daily mean discharge at the Little Falls gage. The NO_3^- concentrations in groundwater ($NO_3^-{}_{GWD}$) and runoff ($NO_3^-{}_{RO}$) were calculated by assuming that $NO_3^-{}_{proc}$ was minimal during winter when river temperature was <5°C. A linear least squares regression was then developed between Q_{GWD} and $NO_3^-{}_{meas}$ for these winter conditions in the river. This relationship was highly significant ($p < 0.001$) with $r^2 = 0.52$, providing confidence that this winter relationship reflects the mixing of 2 sources with little attenuation from in-stream processing. In contrast, similarly derived linear regression relations for the other seasons had $r^2 < 0.07$, suggesting that stream processing of NO_3^- in the river during the nonwinter seasons does not simply reflect the mixing of 2 NO_3^- sources. $NO_3^-{}_{GWD}$ was obtained from the winter regression for $Q_{GWD} = Q_{stream}$, and $NO_3^-{}_{RO}$ was obtained for $Q_{GWD} = 0$. Equation 3 was then solved for $NO_3^-{}_{in}$, which represents the NO_3^- concentration in water transported to the river prior to any effects of in- or near-stream processing, just outside the zone of hyporheic mixing. $NO_3^-{}_{meas}$ was then subtracted from $NO_3^-{}_{in}$ to estimate the increase or decrease in NO_3^- concentration attributable to the net effects of in- or near-stream biogeochemical processing throughout the basin. This daily change in NO_3^- concentration caused by in-stream processing is equivalent to a NO_3^- mass when multiplied by daily mean Q.

The loss of potential NO_3^- load from in- and near-stream processes was compared to the loss of NO_3^- from diel processes. However, these losses apply to different parts of the river network. The approach of Miller et al. (2016) calculates NO_3^- loss applicable to the entire reach length of the river network (252 km during their study). In contrast, the 1-d travel distance that is the dominant influence on diel NO_3^- loss is on the order of 40 to 50 km at moderate flow (Searcy and Davis 1961), a 5- to 7-fold shorter distance. The estimated 1-d travel distance during our study is reported in the Results section of this paper. Additional details about this method and its assumptions were published by Miller et al. (2016).

RESULTS

General patterns with season and storms

NO_3^- concentrations showed a distinct seasonal pattern in the Potomac River with peak values of ~2 mg/L in winter, declining concentrations through spring and summer, and annual minimum concentrations of ~0.5 mg/L in late summer to autumn (Fig. 3A). Superimposed on the seasonal NO_3^- pattern were excursions typically driven by rain events and the associated response at high flows. NO_3^- concentrations commonly decreased during the hydrograph rise and then increased and peaked early in the recession, but this pattern varied with season and the size of the event. At the scale of 2 y, diel NO_3^- concentration patterns are not readily apparent (Fig. 3A). However, these patterns emerge when shorter periods are examined. For example, diel NO_3^- variation was apparent from 3 to 9 May 2013 (Fig. 3B). A rain event that resulted in increased Q beginning 9 May illustrates how diel NO_3^- patterns were disrupted by storms with NO_3^- dilution during peak flow (some data are missing)

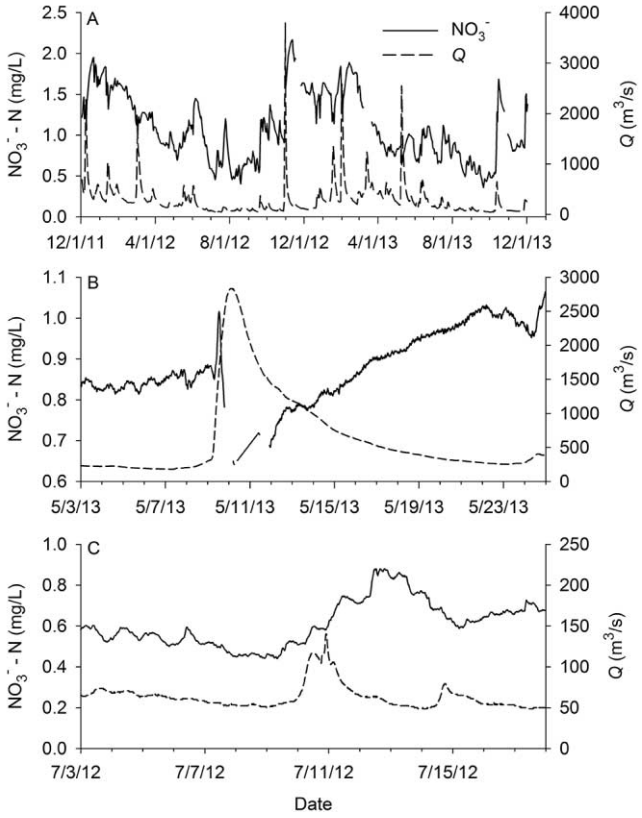

Figure 3. Nitrate (NO_3^-) and discharge (Q) in the Potomac River at Little Falls from December 2011 to November 2013 (A), 3–24 May 2013 (B), and 3–17 July 2012 (C). Dates are formatted mm/dd/yy.

and a gradual increase during recession. A pattern of diel variation appeared to re-establish itself on 22 May, nearly 2 wk after the storm, but then dissipated as NO_3^- concentrations increased again in association with a small hydrograph rise on 24 May. Another rain event during July 2012 showed a different pattern. NO_3^- concentrations increased and peaked ~2 d after the hydrograph (Fig. 3C). This storm led to a smaller response in NO_3^- concentrations and Q than did the May 2013 storm, and the diel NO_3^- pattern generally persisted except for a period ~1 to 2 d after the hydrograph peak. These examples highlight the observed variation in diel patterns and the need to exclude data mainly from large storms when non-diel patterns of variation are dominant. A diel signal was generally not evident after large storms and, therefore, could not be quantified in our analysis.

Magnitude of diel NO_3^- concentration loss

Daily decreases in NO_3^- concentrations that may be attributable to a variety of processes, such as assimilation and denitrification, are here termed 'diel losses', and mean and maximum values of diel loss were calculated for each day of the 24-mo study period (Fig. 4A). Daily mean diel loss values ranged from ~0.01 mg N/L in winter to 0.02 to 0.03 mg N/L in summer and peaked in July of each year. The exception to this pattern was in December 2012 when the highest monthly mean diel loss value of ~0.04 mg N/L was recorded. This range of variation is well within the ability of the sensor to detect change based on the short-term precision of 0.004 mg/L, which we attempted to further enhance by using a 5-measurement moving average. The daily maximum diel loss value generally was ~2× the daily mean loss value, and the seasonal patterns of these 2 quantities were nearly identical (Fig. 4A). As a percentage of the cumulative daily $NO_3^-{}_{max} - NO_3^-{}_i$ concentration, diel loss ranged from <1% in winter to ~2 to 4% in summer and peaked in July of each year (Fig. 4B). Again, December 2012 was anomalously high on a seasonal % basis, with a daily mean diel loss of ~3%. The % daily maximum diel NO_3^- loss values were ~2× those calculated on a daily mean basis.

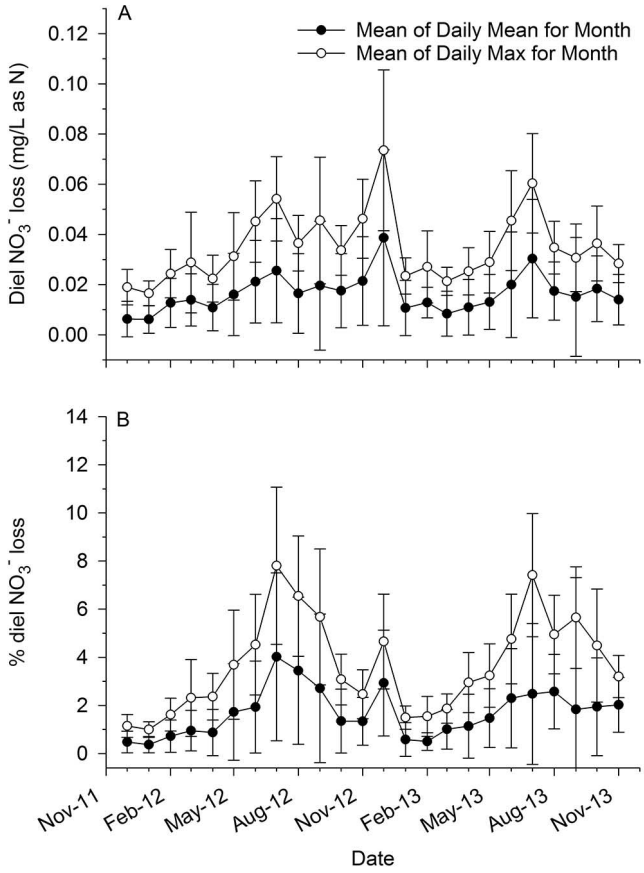

Figure 4. Mean (±SD) daily diel NO_3^- loss and daily maximum diel NO_3^- loss expressed as mg N/L (A) and as % daily mean NO_3^- concentration (B) in the Potomac River at Little Falls for each month during December 2011–November 2013. Dates are formatted month-yy. Max = maximum, min = minimum.

Timing of diel NO_3^- concentration maxima and minima

In summer, maximum diel NO_3^- concentrations generally occurred during late morning, and minimum diel values occurred in the early evening (Fig. 5A). A small secondary peak in maximum diel NO_3^- concentrations also was evident at ~0300 h in summer. In spring, the maximum diel NO_3^- concentrations occurred most often at 0930 h, earlier than the summer value of 1100 h. The minimum diel NO_3^- concentration occurred most often at 1630 h in spring, similarly earlier than the summer value of 1945 h. The predawn secondary peak in maximum diel NO_3^- concentrations was barely evident in spring. The greater *z* scores for maximum and minimum diel NO_3^- concentrations in summer than in spring indicate that more summer than spring days followed the dominant diel pattern.

In autumn, maximum diel NO_3^- concentrations tended to occur in the morning with a fairly broad peak centered at 0730 h (Fig. 5B). The minimum diel NO_3^- concentrations in autumn showed a broad and indistinct range that extended from late afternoon through midnight. The pattern in winter showed 2 diel NO_3^- peaks at 2400 and 0945 h and 2 minima at 0415 and 1500 h. This pattern does not necessarily indicate that 2 maxima and minima occurred on a daily basis, but rather that timing varied from day to day, and that these 2 maxima and minima times were the most common in winter. In general, the mean *z* scores indicate that autumn (maximum = 0.31, minimum = –0.27) and winter (maximum = 0.37, minimum = –0.32) showed less tendency for repeated occurrence of a single maximum and minimum diel NO_3^- concentration than did spring (maximum = 0.41, minimum = –0.37) and summer (maximum = 0.65, minimum = –0.70).

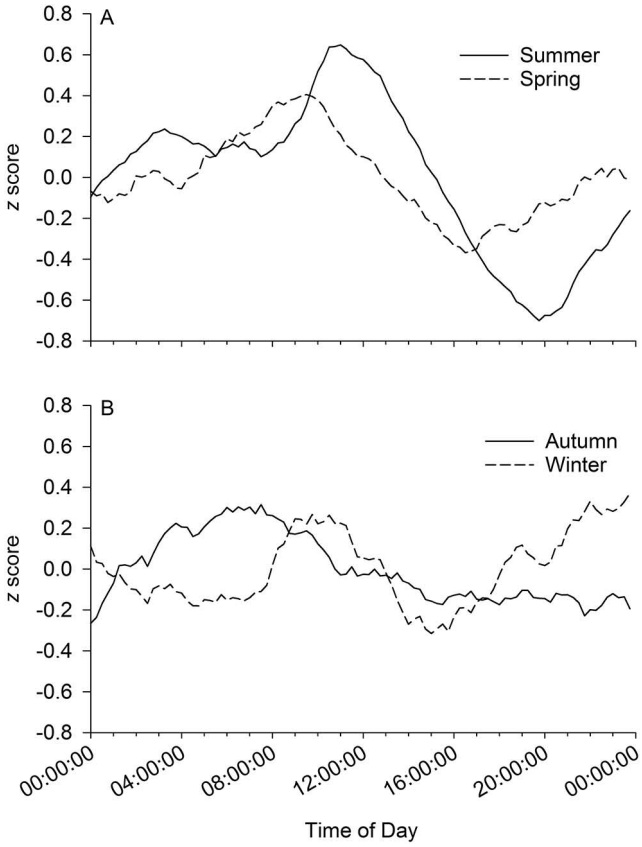

Figure 5. Mean *z* score for NO_3^- concentrations by time of day in spring (21 March–20 June) and summer (21 June–20 September) (A) and in autumn (21 September–20 December) and winter (21 December–20 March) (B). Values are normalized as *z* scores by subtracting the NO_3^- concentration for each 15 min measurement from the daily mean value derived from the Loess smooth and dividing by the standard deviation of the smooth mean. Time of day is formatted as hh:mm:ss.

Relationships of diel NO_3^- concentration amplitude and timing to physical measures

The physical measures that showed the strongest associations with diel NO_3^- loss and timing are shown in Table 1 (see Table S1 for complete results). Among all physical measures that were explored, daily mean water temperature generally showed the strongest association with diel NO_3^- loss magnitude and timing, and the relationships generally were highly significant ($p < 0.001$) except for the time of diel NO_3^- minima. These associations were generally positive, indicating greater NO_3^- loss as temperature increased.

Measures derived from *Q* generally showed the next strongest associations with diel NO_3^- loss and timing, and PAR measures generally showed the weakest associations with a few exceptions (Table 1). Diel NO_3^- loss was inversely related to daily *Q* and 7-, 10-, and 14-d antecedent *Q*. Antecedent 14-d PAR was positively related to diel NO_3^- loss.

Among the diel NO_3^- loss metrics, % mean loss and % maximum loss generally showed the strongest associations with the physical measures, whereas the timing of maxima and minima showed the weakest associations (Table 1). The daily diel NO_3^- mean and maximum loss metrics (mg/L and %) showed similar correlation strengths with the physical measures, but the maximum values always showed slightly stronger correlations.

Exploration of these diel NO_3^- loss metrics through multiple linear regression showed that various combinations of water temperature, *Q*, and PAR could account for 21 and 25% of the variation in mean and maximum diel NO_3^- loss, respectively, and 43 and 53% of the variation in mean and maximum % diel NO_3^- loss, respectively (Table S2). The best models included 3 to 5 dependent variables and always had water temperature as the strongest explanatory variable. Regression models with larger numbers of predictive variables had unacceptably high autocorrelation (variance inflation factor > 6) or explained little additional variation in the diel NO_3^- metrics. This effort was intended to be explo-

Table 1. Pearson product moment correlations for daily metrics of diel NO_3^- loss in the Potomac River and physical measures of water temperature, discharge (Q), and photosynthetically active radiation (PAR). Analysis is based on 537 daily values from December 2011 to November 2013. The measures shown are those with the strongest relationship to diel NO_3^- loss among a larger group of variables that were explored. Correlations of variables with daily loss and maximum daily loss were significant ($p < 0.05$) when $r > |0.09|$ and highly significant ($p < 0.001$) when $r > |0.145|$. Correlations of time of daily maximum and minimum were calculated with a circular statistics approach. Variables for these correlations were significant when $r > 0.109$ and highly significant when $r > 0.161$.

Metric of diel NO_3^- loss	Water temperature (°C)	14-d antecedent Q (m^3/s)	10-d antecedent Q (m^3/s)	Q (m^3/s)	7-d antecedent Q (m^3/s)	14-d antecedent PAR (W/m^2)
Daily loss (mg/L)	0.294	−0.299	−0.270	−0.268	−0.228	0.157
% daily loss	0.598	−0.490	−0.456	−0.422	−0.406	0.445
Maximum daily loss (mg/L)	0.343	−0.323	−0.299	−0.278	−0.258	0.205
% maximum daily loss	0.672	−0.526	−0.493	−0.442	−0.441	0.528
Time of daily maximum	0.262	0.206	0.205	0.182	0.208	0.207
Time of daily minimum	0.122	0.177	0.171	0.154	0.157	0.135

ratory to provide an indication of the predictive ability of variables that might explain the seasonal variation in these NO_3^- data. Therefore, the models are not described or discussed in detail here (see Table S2).

Magnitude of load loss from diel variation in NO_3^- concentrations compared to total in-stream load loss estimates

Data from the NO_3^- sensor at Little Falls were applied in combination with a hydrograph separation approach to estimate NO_3^- concentrations that represented the integrated groundwater and runoff NO_3^- contribution to the river. The sum of the groundwater and runoff NO_3^- mass contributions minus the river NO_3^- load provided an estimate of total in-stream NO_3^- loss during transport in the river network. The mean total NO_3^- loss for the 2-y study period was estimated to be 33.6% of the potential NO_3^- load, and this value ranged from 2.8% during winter to 56.0% during summer with intermediate values during spring and autumn (Table 2). The NO_3^- loss at Little Falls attributed to diel variation was considerably less than the total in-stream loss with values that ranged from 0.7% of the NO_3^- load during winter to 3.0% in summer. Even the maximum NO_3^- diel loss rate ranged from only 1.5% to 6.3% seasonally, still considerably less than the total in-stream loss.

Estimates of areal NO_3^- loss rates

Areal diel NO_3^- loss rates generally ranged (interquartile range) from ~800 to 2300 mg N m^{-2} d^{-1} during all seasons, with only slight differences in values across the seasons (Fig. 6). Mean loss rates were ~1500 to 1900 mg N m^{-2} d^{-1} and median values were ~1200 to 1600 mg N m^{-2} d^{-1}. Mean and median loss rates were highest in summer and lowest in winter (mean) or autumn (median). The broadest range between mean and median values and the

Table 2. Mean (±SD) estimates of total in-stream NO_3^- loss, daily mean diel NO_3^- loss, and daily maximum diel NO_3^- loss in the Potomac River at Little Falls from December 2011 to November 2013 by season and for the complete study period as a percentage of the stream NO_3^- load.

Season	Total in-stream NO_3^- loss (% of load)	Daily mean diel NO_3^- loss (% of load)	Daily maximum diel NO_3^- loss (% of load)	1-d travel reach length (km)
Winter	2.8 ± 11.2	0.7 ± 0.4	1.5 ± 0.7	55.8 ± 10.6
Spring	40.7 ± 10.5	1.5 ± 1.0	3.1 ± 1.6	51.5 ± 12.7
Summer	56.0 ± 11.1	3.0 ± 1.6	6.3 ± 2.7	37.1 ± 3.4
Autumn	25.4 ± 28.1	1.8 ± 1.1	3.6 ± 2.0	41.7 ± 14.1
Total	33.6 ± 25.1	1.8 ± 1.4	3.8 ± 2.6	46.0 ± 3.1

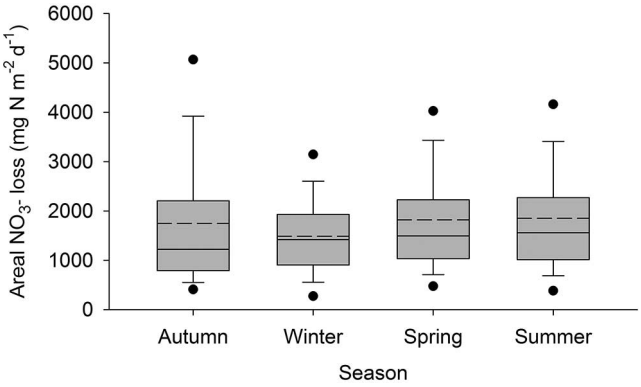

Figure 6. Box-and-whisker plot showing seasonal estimates of areal NO_3^- loss rates in the Potomac River at Little Falls. Lines in boxes are medians, dashed lines are means, box ends are quartiles, whiskers are the 90th and 10th percentile of data, and filled circles are 95th and 5th percentiles.

highest 95th percentile value occurred in autumn, the most skewed distribution among the seasons. These high values generally occurred during December 2012, an unusually warm, sunny, and low-flow period.

DISCUSSION

The data analysis methods and derived quantities developed and applied here, such as NO_3^- loss, are intended to provide estimates that characterize and reflect diel NO_3^- variation patterns and allow comparisons to river sites where high-frequency measurements of NO_3^- and other variables, such as temperature and *Q*, are available. The Little Falls site did not have a dissolved O_2 (DO) sensor operating during the analysis period (high frequency DO measurements began in late 2013), and thus, measures of stream metabolism could not be estimated and compared with estimates of NO_3^- loss. However, even if available, high-frequency measurements of DO and NO_3^- at one site in a heterogeneous river setting, such as that of the Potomac River, violate many of the assumptions for calculating measures of stream metabolism (Reichert et al. 2009), which probably necessitate measurements at ≥2 sites along a reach with better constrained conditions. Nonetheless, our analysis provides insight into seasonal patterns in the magnitude and timing of diel NO_3^- variation in the Potomac River, how strongly diel variation was related to physical factors that may serve as drivers, comparison of diel NO_3^- variation with total river network in-stream NO_3^- loss estimates, and seasonal patterns of NO_3^- loss rates.

Despite broad seasonal and storm-driven variation in NO_3^- concentrations in the Potomac River, clear diel NO_3^- variation also was evident in this ~30,000 km^2 basin, especially at low flow and during summer. A tendency for disruption of the diel NO_3^- pattern during storms was noted, with a gradual recovery of this pattern during hydrograph recession, which has been observed previously in other systems (Reilly et al. 2000) and interpreted as representing the effects of post-flood ecological succession (Grimm 1987). The diel pattern tended to persist during storms that resulted in only a small hydrograph rise. Our analysis and available data cannot be used to determine unequivocally the dominant processes responsible for the diel NO_3^- concentration patterns observed and quantified in the Potomac River. Previous investigators have identified a large range of mechanisms that can result in diel variation including: autotrophic assimilation by periphyton and macrophytes (Grimm 1987, Heffernan and Cohen 2010), indirect effects of assimilation on denitrification through the availability of labile C (Heffernan and Cohen 2010) or DO (Christensen et al. 1990, Holmes et al. 1996), cycling between nitrification and denitrification driven by the availability of DO (Laursen and Seitzinger 2004), and effects of evapotranspiration on transporting NO_3^- from groundwater adjacent to the channel (Flewelling et al. 2014, Duncan et al. 2015). Some combination of these processes may act in concert to produce the observed diel signal, especially in the large heterogeneous Potomac River basin. In addition, hydraulic factors, such as hydrologic dispersion, transient storage, contributions from tributaries that are not temporally synchronized with the river, and anthropogenic discharges can influence the presence/absence of a diel solute signal and the timing and magnitude of that signal (Hensley and Cohen 2016).

Magnitude of diel NO_3^- variation

The magnitude of diel variation in the river generally was not large (<1% of the daily mean NO_3^- concentration in winter and ~2 to 4% of this value in summer), although values >10% were observed on some days in summer. This range of relative variation is generally less than that reported for many smaller streams and rivers (Mulholland 1992, Heffernan and Cohen 2010, Halliday et al. 2013, Flewelling et al. 2014). Even when the maximum diel loss values were applied rather than the mean values as above, diel NO_3^- variation generally peaked at ~8% in July of each year.

Diel NO_3^- loss diminished stream loads on average by a range of 0.7% in winter to 3% in summer. Percent load losses reached values >5% on some summer days. These values represent losses of NO_3^- at low and moderate flow. The extent to which diel processes may have diminished loads during storms is not known because diel patterns could not be identified in these high-flow data.

The diminishment of NO_3^- loads by diel processes was much less than estimated total losses of NO_3^- (except during winter) throughout the Potomac River basin from all in-stream and near-stream processes, which ranged from 2.8% in winter to 56% in summer. However, these total NO_3^- losses represent those that occurred throughout the whole basin channel network (mean reach length =

252 km), whereas the values from our analysis primarily represent those that occurred within a 1-d travel time upstream of the Little Falls gage, a mean reach length of 46 km (Table 2). The maximum NO_3^- load losses that could be attributed to diel-driven processes were in the range of 7 to 13× less than those calculated for the total in-stream river-network NO_3^- load losses during the nonwinter seasons (Table 2), which were less than the 5.5-fold difference in mean reach lengths for the 2 methods. This indicates that non-diel-driven processes probably are important in diminishing in-stream NO_3^- concentrations during transport in the Potomac River. A more complete quantitative assessment of the basin-wide role of diel-driven NO_3^- loss rates would require multiple analyses across a range of sites with varying basin areas.

Our results suggest that much of the near-stream and in-stream removal or retention of NO_3^- may occur either through hyporheic exchange or as groundwater discharges to the stream network in the Potomac basin via processes that are not reflected in the diel variation of NO_3^- concentrations measured at Little Falls. Much NO_3^- removal in the near-stream environment may occur either through vertical hyporheic exchange driven by hydrogeomorphic variation in the channel (Gomez-Velez et al. 2015) or through denitrification as inflowing groundwater enters through deeper sediment (Stelzer and Bartsch 2012, Lansdown et al. 2015). Both of these processes may be minimally influenced by diel variation in processes such as photoautotrophy. The data presented here are consistent with these observations that much in-stream NO_3^- loss in the Potomac River may not be greatly influenced by diel-driven processes. However, this statement must be qualified by emphasizing that the true diel losses of NO_3^- that may have resulted from various biogeochemical processes may be larger than the values quantified in our analysis because of the unknown role of various hydraulic factors that may partially obscure the diel signal (Hensley and Cohen 2016).

Timing of diel NO_3^- patterns

The timing of the diel maxima and minima differs from the patterns reported by many authors in which the maximum value typically occurs at night in predawn hours and the minimum value in mid-afternoon (Mulholland et al. 2006, Heffernan and Cohen 2010, Halliday et al. 2013). However, widely varying patterns have been reported that may reflect complex daily dynamics in evapotranspiration (and near-stream ground water), pH, water temperature, or agricultural water management practices (Laursen and Seitzinger 2004, Pellerin et al. 2009, Flewelling et al. 2014). A recent modeling investigation demonstrated that the daily minima in NO_3^- concentrations can lag behind solar forcing because of transport processes and that water arriving at a measurement location reflects the effects of cumulative rather than instantaneous processes (Hensley and Cohen 2016). The timing of the diel maxima and minima observed in the Potomac River did not coincide with daylight in a simplistic manner in any season. The maximum diel NO_3^- concentration typically occurred from early to late morning, except for winter when a midnight peak was co-dominant with a mid-morning peak. Similarly, the minimum diel NO_3^- concentration tended to occur between late afternoon and early evening, lagging the peak sunlight hours. In addition, the maxima and minima in autumn and winter had lower mean z scores indicating less persistent patterns in these seasons. In contrast, the z scores in spring and particularly in summer were more persistent indicating higher repeatability of the maxima and minima. These seasonal differences may be explained in part by seasonal patterns in incident solar radiation. Mean PAR values in autumn and winter were 180.7 μmol m^{-2} s^{-1} and 183.3 μmol m^{-2} s^{-1}, respectively, whereas these mean values were 386.7 μmol m^{-2} s^{-1} in spring and 403.1 μmol m^{-2} s^{-1} in summer. The greater PAR values in spring and summer may have led to stronger persistence in the timing of the daily maxima and minima, whereas in winter, other factors, such as variation in water temperature and Q, may have played a stronger role in causing greater variation in the day-to-day timing of the maxima and minima.

The differences in timing across seasons suggest that a complex mix of processes may be responsible for the observed variation. Two of these processes are hydrodynamic dispersion and transient storage, which can affect both the timing and amplitude of the diel NO_3^- signal (Heffernan and Cohen 2010, Hensley and Cohen 2016). The combined effect of both processes results in a lag of the minima from peak solar forcing (Hensley and Cohen 2016). Dispersion and storage in a given river reach vary in a complex manner with discharge and season as reflected by variation in velocity, depth, width, turbulence, and water temperature (viscosity). The extent to which seasonal variation in hydrodynamic dispersion and transient storage may have affected seasonal variation in the timing of diel NO_3^- maxima and minima is not known.

A critical factor that affects the timing of diel variation (and magnitude) of any water-chemistry variable is the mean in-stream residence time of a parcel of water as it passes the sensor or sampling location (Worrall et al. 2013). The effects of any processes driven by variation in solar radiation are expected to vary because day length, the timing of sunrise and sunset, and V affect the amount of time that a water parcel is exposed to light and dark conditions. These factors are especially critical in small streams where travel times may be a few hours to <1 d, which greatly affects the relative amounts of time a parcel of water has been exposed to light or dark conditions. However, at the scale of the Potomac River at Little Falls, in-stream residence time is likely to be a minor explanatory factor because travel times in the river at this scale are in

the range of 4–14 d (Searcy and Davis 1961), and the relative light vs dark exposure diminishes as residence time increases downstream. *V* estimates applied in our analysis yielded mean basin-wide travel times of 4 to 6 d during the December 2011 to November 2013 study period, indicating that river water was exposed to several days of the processes that drive diel variation before reaching the Little Falls stream gage. This result suggests that the diel variation in NO_3^- concentrations observed at the scale of Little Falls primarily should reflect the most recent 24 h. However, hydrodynamic dispersion and transient storage during transport as discussed above also can affect the timing of the diel signal.

Role of physical drivers of diel NO_3^- variation

Among the potential physical drivers that may affect the magnitude and timing of diel variation in NO_3^- concentrations in the Potomac River, water temperature was most strongly related to the daily patterns. Metrics based on PAR generally were not as strongly related to the magnitude and timing of diel NO_3^- patterns as were those based on water temperature, suggesting that these patterns were not simply driven directly by solar radiation as observed in some studies (Mulholland et al. 2006, Heffernan and Cohen 2010). However, water temperature variation has proven the strongest predictor of diel NO_3^- variation in many settings (Laursen and Seitzinger 2004, Birgand et al. 2007). The central role of water temperature as a driver of diel NO_3^- variation may reflect decreased dynamic viscosity of water as temperature increases, which increases saturated hydraulic conductivity and hyporheic exchange in riverbed sediment (Storey et al. 2003). Alternatively, diel NO_3^- variation may be driven largely by increased rates of microbial processes, such as denitrification as water temperature increases (van Kessel 1977).

The strong inverse relationship of metrics based on *Q* with the magnitude of diel NO_3^- variation is consistent with an increasing influence of photoautotrophs during hydrograph recession and low flow. As *Q* increases, organic-rich sediment may be readily scoured from the channel bottom and replaced by sandy sediment, which can promote an inverse relationship between *Q* and denitrification rate (Christensen et al. 1990). The inverse relationship with *Q* also suggests a potential role for dispersion in diminishing NO_3^- variation during high flow. Last, despite the statistical significance of the associations of water temperature, *Q*, and PAR with diel NO_3^- variation, no combination of factors could account for even 1/2 of the diel variation measured. Our inability to build regression models with high explanatory power indicates the likelihood of complex nonlinear interactions of the various processes that affect diel NO_3^- variation in the Potomac River, which were not readily accounted for by simple metrics based on temperature, *Q*, or PAR.

Areal NO_3^- loss rates

The diel areal NO_3^- loss rates estimates were generally in the range of 800 to 2300 mg N m^{-2} d^{-1}, about an order of magnitude greater than those reported in many studies in small streams and rivers (Mulholland et al. 2006, Heffernan and Cohen 2010, Halliday et al. 2013), comparable to those reported in some rivers (Peterson et al. 2001), but less than those reported at a few sites (Laursen and Seitzinger 2004). In a review of published NO_3^- removal rates in streams, ~1/2 of the reported rates were <350 mg N m^{-2} d^{-1}, and <20% were >1000 mg N m^{-2} d^{-1} (Birgand et al. 2007). Thus, the diel areal NO_3^- loss rates in the Potomac River are greater than most previously reported rates. This result is especially surprising because the values reported here are not total loss rates, but just the fraction that can be attributed to diel variation. However, an examination of literature values shows that most of the published rates are from streams and rivers considerably smaller than the ~30,000 km^2 Potomac River basin. Equation 1 shows that the fundamental controls on the diel areal loss rate of NO_3^- are the magnitude and temporal extent of the daily dip in NO_3^- concentrations and the depth of the water column. The term Q/WV in Eq. 1 represents the depth of the water column above each square meter of channel bottom. As a consequence, diel areal loss rates will be greater for a similar dip in NO_3^- concentrations in a large river than in a smaller river or stream. Thus, the most meaningful comparisons of the areal loss rates calculated here are among similarly sized rivers. However, few values are available from river systems comparable to the Potomac.

Only slight seasonal variability was identified in the diel areal NO_3^- loss rates estimated in our study. For example, the highest seasonal mean rate in summer was just 24% greater than the lowest seasonal mean rate in winter. This result may seem surprising because most previous investigators have found substantially higher rates in spring or summer than in winter (Mulholland et al. 2006, Birgand et al. 2007). However, mean river depth in winter was ~2× that in summer on days for which rates were estimated. Therefore, a diel NO_3^- concentration loss in winter that is 1/2 that of summer, would result in a similar diel areal loss rate if summer river depth were 1/2 that of winter. This seasonal variation in *Q* and river depth effectively smoothes some of the seasonal differences that were evident in diel NO_3^- concentration and load losses when rates are calculated on an areal basis.

Unusually high diel NO_3^- variation in December 2012

The mean diel variation in NO_3^- concentrations in December 2012 was ~0.04 mg/L, the highest of any month during the study period. The magnitude of this variation seems especially surprising considering the short day length and cold river temperatures in late autumn. This period of

unusually high diel NO_3^- variation extended from 30 November to 19 December. A comparison of some physical measures during this period with those of the succeeding month, January 2013, and December 2011 suggests some reasons for such high diel variation in NO_3^- concentrations in December 2012 (Fig. 7). PAR was similar among these 3 periods, but mean water temperature was ~7.5°C between 30 November and 19 December 2012, ~6°C in December 2011, and 3.5°C in January 2013. *Q* showed the greatest difference among these 3 periods. *Q* was ~4- to 5-fold less during the December 2012 period of high diel NO_3^- variation than during the other 2 periods and was steady with little daily variation. Mean *Q* during December 2012 (115 m^3/s) was similar to the mean summer value during our study (103 m^3/s). These data suggest that the extended period of low river flow, perhaps combined with warmer river temperatures, may have favored greater diel NO_3^- variation than expected during December 2012. These data indicate that extended periods of low and stable flow can result in a strong diel NO_3^- pattern, even when day length and PAR were near their lowest levels of the year.

Conclusions

High frequency sensor measurements revealed strong seasonal and flow-related patterns of variation in NO_3^- concentrations in the Upper Potomac River at a basin scale of 30,000 km^2. Within these broader patterns was clear and repeatable diel variation in NO_3^- concentrations in the river that was especially evident during periods of low and moderate flow. This diel NO_3^- variation ranged from daily mean values of 0.01 mg N/L in winter to 0.02 to 0.03 mg N/L in summer with intermediate values in spring and autumn. NO_3^- concentrations generally showed maximum diel values in mid- to late-morning and minimum diel values in late afternoon to early evening with less distinct maxima and minima in autumn and winter. The range of diel variation reached maximum summer values equivalent to only ~8% of the daily $NO_3^-{}_{max}$ concentration. However, the mean estimated areal diel NO_3^- loss rate was quite high, and ranged from ~800 mg N m^{-2} d^{-1} to 2300 mg N m^{-2} d^{-1} throughout the year with slight seasonal variation. These areal loss rates are generally greater than most rates reported in the literature, which are mainly from streams and small rivers. These relatively high areal loss values reflect that the Potomac is a 7th-order river that integrates diel NO_3^- losses over a greater depth/unit of channel bottom area than that of smaller streams and rivers. The proportion of the potential river NO_3^- load that was removed through diel loss in the study reach ranged from 0.7% in winter to 3% in summer, much less than whole-basin annual loss rates of ~33% of the NO_3^- load calculated by an independent method that considers all in-stream and near-stream losses of NO_3^- discharged to the river from ground water. These diel load losses cannot account for a substantial proportion of the total basin in-stream load losses reflecting in part, the shorter 1-d reach length but also suggesting that processes not driven by diel variation are responsible for much of the in-stream load loss in the Potomac River.

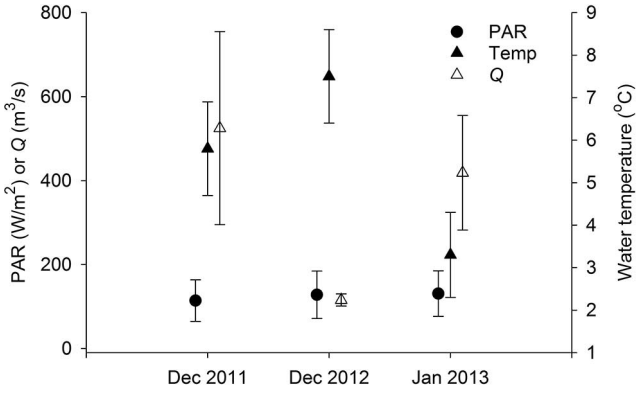

Figure 7. Mean (±SD) photosynthetically active radiation (PAR), water temperature (Temp), and discharge (*Q*) in the Potomac River at Little Falls in December 2011, from 30 November to 19 December 2012, and in January 2013.

The extent to which diel NO_3^- variation was damped by hydrologic dispersion and transient storage would have to be quantified to constrain our estimate fully. More spatially detailed measurements of *W*, depth, *V*, and *Q* along the reach, which generally influence diel NO_3^- variation also would help to better constrain the loss rate estimates presented here. In addition, the roles of several variables that may serve as drivers, covariates, or links in the N cycle, such as DO or dissolved organic N, for which high-frequency measurements were not available, are not well known. Furthermore, the conclusions that can be drawn from this analysis of high-frequency measures of NO_3^-, *Q*, water temperature, and PAR could be further constrained by applying a 2-station approach focused on intensive measurements along a stream reach that included DO, NH_4^+, and organic N. Accompanying measurements of ground water, the hyporheic zone, and sediment chemical gradients could improve understanding of the physical and biogeochemical processes that affect diel NO_3^- loss in the Potomac River. The approach and description/quantification of diel NO_3^- variation provided here can serve as a framework for estimates of seasonal and annual patterns that may be applied at other river sites where high-frequency NO_3^- sensor data are available.

ACKNOWLEDGEMENTS

Author contributions: DAB wrote most of the manuscript and performed most of the data analyses. MPM developed the method and provided guidance for estimating total in-stream NO_3^- loss. BAP performed quality assurance/quality control on

NO_3^- sensor data and wrote the sensor measurements subsection. PDC, MPM, and BAP offered constructive suggestions on various drafts of the manuscript.

Funding for this work was provided by the US Geological Survey National Water-Quality Assessment Program. Use of brand names is for identification purposes only and does not imply endorsement by the US Geological Survey.

LITERATURE CITED

Alexander, R. B., R. A. Smith, and G. E. Schwarz. 2000. Effect of stream channel size on the delivery of nitrogen to the Gulf of Mexico. Nature 403:758–761.

Ator, S. W., J. D. Blomquist, J. W. Brakebill, J. M. Denis, M. J. Ferrari, C. V. Miller, and H. Zappia. 1997. Water quality in the Potomac River basin, Maryland, Pennsylvania, Virginia, West Virginia, and the District of Columbia, 1992–96. Circular 1166. US Geological Survey, Reston, Virginia.

Ator, S. W., J. H. Brakebill, and J. D. Blomquist. 2011. Sources, fate, and transport of nitrogen and phosphorus in the Chesapeake Bay Watershed: an empirical model. Scientific-Investigations Report 2011-5167. US Geological Survey, Reston, Virginia.

Birgand, F., R. W. Skaggs, G. M. Chescheir, and J. W. Gilliam. 2007. Nitrogen removal in streams of agricultural catchments—a literature review. Critical Reviews in Environmental Science and Technology 37:381487.

Blomquist, J. D., G. T. Fisher, J. M. Denis, J. W. Brakebill, and W. H. Werkheiser. 1996. Water quality assessment of the Potomac River: basin description and analysis of available nutrient data, 1970-90. Water-Resources Investigations Report 95-4221. US Geological Survey, Towson, Maryland.

Boynton, W. R., J. H. Garber, R. Summers, and W. M. Kemp. 1995. Inputs, transformations, and transport of nitrogen and phosphorus in Chesapeake Bay and selected tributaries. Estuaries 18:285–314.

Bricker, S. B., B. Longstaff, W. Dennison, A. Jones, K. Boicourt, C. Wicks, and J. Woerner. 2008. Effects of nutrient enrichment in the nation's estuaries: a decade of change. Harmful Algae 8:21–32.

Bricker, S. B., K. C. Rice, and O. P. Bricker. 2014. From headwaters to coast: influence of human activities on water quality of the Potomac River Estuary. Aquatic Geochemistry 20:291–323.

Burns, D. A. 1998. Retention of NO_3^- in an upland stream environment: a mass balance approach. Biogeochemistry 40:73–96.

Christensen, P. B., L. P. Neilsen, J. Sorensen, and J. P. Revsbach. 1990. Denitrification in nitrate-rich streams: diurnal and seasonal variation related to benthic oxygen metabolism. Limnology and Oceanography 35:640–651.

Cleveland, W. S., and S. J. Devlin. 1988. Locally weighted regression: an approach to regression analysis by local fitting. Journal of the American Statistical Association 83:596–610.

Collischonn, W., and F. M. Fan. 2013. Defining parameters for Eckhardt's digital baseflow filter. Hydrological Processes 27: 2614–2622.

Duncan, J. M., L. E. Band, P. M. Groffman, and E. S. Bernhardt. 2015. Mechanisms driving the seasonality of catchment scale nitrate export: evidence for riparian ecohydrologic controls. Water Resources Research 51:3982–3997.

Eckhardt, K. 2005. How to construct recursive digital filters for hydrograph separation. Hydrological Processes 19:507–515.

Eshleman, K. N., R. D. Sabo, and K. M. Klein. 2013. Surface water quality is improving due to declining atmospheric N deposition. Environmental Science and Technology 47:12193–12200.

Flewelling, S. A., G. M. Hornberger, J. S. Herman, A. L. Mills, and W. M. Robertson. 2014. Diel patterns in coastal-stream nitrate concentrations linked to evapotranspiration in the riparian zone of a low-relief, agricultural catchment. Hydrological Processes 28:2150–2158.

Galloway, J. N., J. D. Aber, J. W. Erisman, S. P. Seitzinger, R. W. Howarth, E. B. Cowling, and B. J. Cosby. 2003. The nitrogen cascade. BioScience 53:341–356.

Galloway, J. N., A. R. Townsend, J. W. Erisman, M. Bekunda, Z. Cai, J. R. Freney, L. A. Martinelli, S. P. Seitzinger, and M. A. Sutton. 2008. Transformation of the nitrogen cycle: recent trends, questions, and potential solutions. Science 320: 889–892.

Gomez-Velez, J. D., J. W. Harvey, B. Y. Cardenas, and B. Kiel. 2015. Denitrification in the Mississippi River network controlled by flow through river bedforms. Nature Geoscience 8:941–945.

Grimm, N. B. 1987. Nitrogen dynamics in a desert stream. Ecology 68:1557–1170.

Hall, R. O., J. L. Tank, D. J. Sobota, P. J. Mulholland, J. M. O'Brien, W. K. Dodds, J. R. Webster, H. M. Valett, G. C. Poole, B. J. Peterson, J. L. Meyer, W. H. McDowell, S. L. Johnson, S. K. Hamilton, N. B. Grimm, S. V. Gregory, C. N. Dahm, L. W. Cooper, L. R. Ashkenas, S. M. Thomas, R. W. Sheibley, J. D. Potter, B. R. Niederlehner, L. T. Johnson, A. M. Helton, C. M. Crenshaw, A. J. Burgin, M. J. Bernot, J. J. Beaulieu, and C. P. Arango. 2009. Nitrate removal in stream ecosystems measured by ^{15}N addition experiments: total uptake. Limnology and Oceanography 54:653–665.

Halliday, S. J., R. A. Skeffington, A. J. Wade, C. Neal, B. Reynolds, D. Norris, and J. W. Kirchner. 2013. Upland streamwater nitrate dynamics across decadal to sub-daily timescales: a case study of Plynlimon, Wales. Biogeosciences 10:8013–8038.

Heffernan, J. B., and M. J. Cohen. 2010. Direct and indirect coupling of primary production and diel nitrate dynamics in a subtropical spring-fed river. Limnology and Oceanography 55:677–688.

Hensley, R. T., and M. J. Cohen. 2016. On the emergence of diel solute signals in flowing waters. Water Resources Research 52:759–772.

Holmes, R. M., J. B. Jones, S. G. Fisher, and N. B. Grimm. 1996. Denitrification in a nitrogen-limited stream ecosystem. Biogeochemistry 33:125–146.

Kemp, W. M., W. R. Boynton, J. E. Adolf, D. F. Boesch, W. C. Boicourt, G. Brush, J. C. Cornwell, T. R. Fisher, P. M. Glibert, J. D. Hagy, L. W. Harding, E. D. Houde, D. G. Kimmel, W. D. Miller, R. I. E. Newell, M. R. Roman, E. M. Smith, and J. C. Stevenson. 2005. Marine Ecology Progress Series 303:1–29.

Lansdown, K., C. M. Heppell, M. Trimmer, A. Binley, A. L. Heathwaite, P. Byrne, and H. Zhang. 2015. The interplay between transport and reaction rates as controls on nitrate attenuation in permeable streambed sediments. Journal of Geophysical Research: Biogeosciences 120:1093–1109.

Laursen, A. E., and S. P. Seitzinger. 2004. Diurnal patterns of denitrification, oxygen consumption, and nitrous oxide production in rivers measured at the whole-reach scale. Freshwater Biology 49:1448–1458.

Lim, K. J., B. A. Engel, Z. Tang, J. Choi, K.-S. Kim, S. Muthukrishnan, and D. Tripathy. 2005. Automated Web GIS based hydrograph analysis tool, WHAT. Journal of the American Water Resources Association 41:1407–1416.

Miller, M. P., A. J. Tesoriero, P. D. Capel, B. A. Pellerin, K. E. Hyer, and D. A. Burns. 2016. Quantifying groundwater loading and in-stream fate of nitrate using high-frequency water quality data. Water Resources Research 52:330–347.

Mulholland, P. J. 1992. Regulation of nutrient concentrations in a temperate forest stream: roles of upland, riparian, and instream processes. Limnology and Oceanography 37:1512–1526.

Mulholland, P. J., R. O. Hall, D. J. Sobota, W. K. Dodds, S. E. G. Findlay, N. B. Grimm, S. K. Hamilton, W. H. McDowell, J. M. O'Brien, J. L. Tank, L. R. Ashkenas, L. W. Cooper, C. N. Dahm, S. V. Gregory, S. L. Johnson, J. L. Meyer, B. J. Peterson, G. C. Poole, H. M. Valett, J. R. Webster, C. P. Arango, J. J. Beaulieu, M. J. Bernot, A. J. Burgin, C. L. Crenshaw, A. M. Helton, L. T. Johnson, B. R. Niederlehner, J. D. Potter, R. W. Sheibley, and S. M. Thomas. 2009. Nitrate removal in stream ecosystems measured by ^{15}N addition experiments: denitrification. Limnology and Oceanography 54:666–680.

Mulholland, P. J., S. A. Thomas, H. M. Valett, J. R. Webster, and J. Beaulieu. 2006. Effects of light on NO_3^- uptake in small forested streams: diurnal and day-to-day variations. Journal of the North American Benthological Society 25:583–595.

National Research Council. 1995. Nitrate and nitrite in drinking water. National Academy Press, Washington, DC.

O'Brien, J. M., and W. K. Dodds. 2010. Saturation of NO_3^- uptake in prairie streams as a function of acute and chronic N exposure. Journal of the North American Benthological Society 29:627–635.

Pellerin, B. A., B. A. Bergamaschi, B. D. Downing, J. F. Saraceno, J. A. Garrett, and L. D. Olsen. 2013. Optical techniques for the determination of nitrate in environmental waters: guidelines for instrument selection, operation, deployment, maintenance, quality assurance, and data reporting. Techniques and Methods 1–D5. US Geological Survey, Reston, Virginia.

Pellerin, B. A., B. A. Bergamaschi, R. J. Gilliom, C. G. Crawford, J. F. Saraceno, C. P. Frederick, B. D. Downing, and J. C. Murphy. 2014. Mississippi River nitrate loads from high frequency sensor measurements and regression-based load estimation. Environmental Science and Technology 48:12612–12619.

Pellerin, B. A., B. D. Downing, C. Kendall, R. A. Dahlgren, T. F. Kraus, J. Saraceno, R. G. Spencer, and B. A. Bergamaschi. 2009. Assessing the sources and magnitude of diurnal nitrate variability in the San Joaquin River (California) with an in situ optical nitrate sensor and dual nitrate isotopes. Freshwater Biology 54:376–387.

Peterson, B. J., W. M. Wollheim, P. J. Mulholland, J. R. Webster, J. L. Meyer, J. L. Tank, E. Martí, W. B. Bowden, H. M. Valett, A. E. Hershey, W. H. McDowell, W. K. Dodds, S. K. Hamilton, S. V. Gregory, and D. D. Morrall. 2001. Control of nitrogen export from watersheds by headwater streams. Science 292:86–90.

Preston, S. D., R. B. Alexander, G. E. Schwarz, and C. G. Crawford. 2011. Factors affecting stream nutrient loads: a synthesis of regional SPARROW model results for the continental United States. Journal of the American Water Resources Association 47:891–915.

Rantz, S. E., and others. 1982. Measurement and computation of streamflow. Volume 1. Measurement of stage and discharge and Volume 2. Computation of discharge. Water-Supply Paper 2175. US Geological Survey, Reston, Virginia.

Reichert, P., U. Uehlinger, and V. Acuña. 2009. Estimating stream metabolism from oxygen concentrations: effect of spatial heterogeneity. Journal of Geophysical Research: Biogeosciences 114:G03016.

Reilly, J. F., A. J. Horne, and C. D. Miller. 2000. Nitrate removal from a drinking water supply with large free surface constructed wetlands prior to groundwater recharge. Ecological Engineering 14:33–47.

Roberts, B. J., and P. J. Mulholland. 2007. In-stream biotic control on nutrient biogeochemistry in a forested stream, West Fork of Walker Branch. Journal of Geophysical Research: Biogeosciences 112:G04002.

Satlantic. 2014. SUNA Manual, SAT-DN-00628, Rev. E, 2014-Dec-01. Satlantic, Halifax, Nova Scotia.

Searcy, J. K., and L. C. Davis. 1961. Time of travel of water in the Potomac River, Cumberland to Washington, DC. Circular 438. US Geological Survey, Washington, DC.

Seitzinger, S. P., R. V. Styles, E. W. Boyer, R. B. Alexander, G. Billen, R. W. Howarth, B. Mayer, and N. Van Breemen. 2002. Nitrogen retention in rivers: model development and application to watersheds in the northeastern USA. Biogeochemistry 57:199–237.

Smith, T. E., A. E. Laursen, and J. R. Deacon. 2008. Nitrogen attenuation in the Connecticut River, northeastern USA: a comparison of mass balance and N_2 production modeling approaches. Biogeochemistry 87:311–323.

Sprague, L. A., M. J. Langland, S. E. Yochum, R. E. Edwards, J. D. Blomquist, S. W. Phillips, G. W. Shenk, and S. D. Preston. 2000. Factors affecting nutrient trends in major rivers of the Chesapeake Bay Watershed. Water-Resources Investigations 00-4218. US Geological Survey, Richmond, Virginia.

Stelzer, R. S., and L. A. Bartsch. 2012. Nitrate removal in deep sediments of a nitrogen-rich river network: a test of a conceptual model. Journal of Geophysical Research: Biogeosciences 117:G02027.

Storey, R. G., K. W. F. Howard, and D. D. Williams. 2003. Factors controlling riffle-scale hyporheic exchange flows and their seasonal changes in a gaining stream: a three-dimensional groundwater flow model. Water Resources Research 39: W1034.

Tank, J. L., E. Rosi-Marshall, M. A. Baker, and R. O. Hall. 2008. Are rivers just big streams? A pulse method to quantify nitrogen demand in a large river. Ecology 89:2935–2945.

Triska, F. J., V. C. Kennedy, R. J. Avanzino, G. Zellweger, and K. E. Bencala. 1989. Retention and transport of nutrients in a third-order stream in northwestern California: hyporheic processes. Ecology 70:1893–1905.

van Kessel, J. F. 1977. Factors affecting the denitrification rate in two sediment–water systems, Water Research 11:259–267.

von Schiller, D., S. Bernal, F. Sabater, and E. Martí. 2015. A round-trip ticket: the importance of release processes for in-stream nutrient spiraling. Freshwater Science 34:20–30.

Wollheim, W. M., C. J. Vörösmarty, B. J. Peterson, S. P. Seitzinger, and C. S. Hopkinson. 2006. Relationship between river size and nutrient removal. Geophysical Research Letters 33: L06410.

Woods, B., J. Walsh, P. Thompson, R. Ashburn, S. Kharkar, N. Passarelli, C. deBarbadillo, R. Derminassian, and D. Dandach. 2013. Filtrate facility at Blue Plains–concept to final design. Proceedings of the Water Environment Federation, Session 54 to 62:1171–1181.

Worrall, F., H. Davies, T. Burt, N. J. K. Howden, M. J. Whelan, A. Bhogal, and A. Lilly. 2012. The flux of dissolved nitrogen from the UK—evaluating the role of soils and land use. Science of the Total Environment 434:90–100.

Worrall, F., N. J. K. Howden, C. S. Moody, and T. P. Burt. 2013. Correction of fluvial fluxes of chemical species for diurnal variation. Journal of Hydrology 481:1–11.

Zar, J. H. 1999. Biostatistical analysis. 4th edition. Prentice-Hall, Upper Saddle River, New Jersey.